Int. J. Heat Mass Transfer. Vol. 17, pp. 1253–1260. Pergamon Press 1974. Printed in Great Britain

DIRECT CONTACT CONDENSATION OF BINARY MIXTURES

A. Tamir,* Y. Taitel† and E. U. Schlünder
Lehrstuhl und Institut für Thermische Verfahrenstechnik, Universität Karlsruhe, West Germany

(*Received* 21 *November* 1973)

Abstract—A boundary-layer analysis of direct contact condensation of binary vapor mixtures on a laminar coolant flowing in a duct is presented. The binary mixture condensate may be immiscible or miscible in the coolant. Both condensable components are, however, assumed completely miscible. The analysis includes also effects of forced convection of the vapor and interfacial resistance at the vapor–liquid interface. The analysis assumes constant properties which are evaluated at an appropriate reference state.

The boundary-layer equations were solved numerically in a transformed coordinate system which admitted a similarity solution for short ducts and when the surface resistance is negligible ($B = \infty$).

The solution is demonstrated for the condensation on water at atmospheric pressure of the immiscible mixture CS_2–CCl_4.

For the case of $B = \infty$ and at the leading edge, the analysis predicts and appreciable reduction in the condensation fluxes as compared to the maximum values obtained when the vapor bulk temperature exists at the interface. This reduction is dependent on the mixture composition and the maximum thermal driving force $(T_\infty - T_0)$. The effect of the forced convection is found appreciable only for relatively small values of $(T_\infty - T_0)$. The effect of the surface resistance is observed to be appreciable near the leading edge. The results indicate also that the similarity solution may be extended up to $\xi = 0{\cdot}1$.

NOMENCLATURE

B,	dimensionless heat-transfer coefficient of the interface, equation (28);
C_p,	heat capacity at constant pressure;
D,	binary diffusivity;
f,	dimensionless stream function;
f_i,	the value of f corresponding to the interface;
$\tilde{f}_i$,	defined in equation (27). Equal to f_i for similarity solution;
h_i,	heat-transfer coefficient of the interface;
k',	thermal conductivity of the coolant stream;
K,	$c'_p\mu\rho'/(k'\rho)$;
L,	coolant stream thickness;
M,	molecular weight;
N,	$\sqrt{[\mu\rho/(c'_p k'\rho')]}\lambda/(T_\infty - T_0)$;
P,	total pressure;
P^0,	partial pressure of the volatile species;
Q,	heat flux in the presence of surface resistance $1/B$, which is defined by the dimensionless temperature gradient $\partial\theta/\partial\tilde{\eta}$ at the interface;
$Q(B = \infty)$,	heat flux in the absence of surface resistance ($B = \infty$);
$Q_\infty(B = \infty)$,	heat flux in the absence of surface resistance and when $T_i = T_\infty$;
Sc,	Schmidt number, $\mu/\rho D$;
T,	local temperature;
T_i,	temperature corresponding to the partial pressure of the volatile component at the interface—"vapor side";
T_w,	surface temperature of the coolant stream;
T_∞,	bulk temperature of the vapor;
u,	longitudinal velocity;
u_w,	value of u at the coolant surface;
u_∞,	free stream velocity;
v,	normal velocity;
V,	dimensionless normal velocity, Lv/α';
w,	mass fraction in the vapor mixture corresponding to the volatile species;
$\bar{w}$,	mass fraction of the volatile species in the condensate;
x,	longitudinal coordinate;
y,	normal coordinate.

Greek symbols

α',	thermal diffusivity of the liquid;
β,	velocity ratio, u_∞/u_w;
γ,	activity coefficient of the volatile species;
η,	coordinate in the vapor phase, equation (12);
$\tilde{\eta}$,	coordinate in the liquid, equation (17);
λ,	latent heat of condensation;
μ,	absolute viscosity, for vapor mixture when used without subscripts;

---

*Present address: Department of Chemical Engineering, University of the Negev, Beer-Sheva, Israel.

†Present address: School of Engineering, Tel-Aviv University, Ramat Aviv, Israel.

ν,	kinematic viscosity;
ξ,	dimensionless axial coordinate, equation (12);
ρ,	density, for vapor mixture when used without subscripts;
θ,	dimensionless temperature, $(T-T_0)/(T_\infty-T_0)$;
ϕ,	w/w_∞;
ψ,	stream function, equation (13).

Subscripts and superscripts

0,	inlet, at $x = 0$;
1,	designates the volatile species (CS_2 in Figs. 2, 4–7);
2,	designates the less volatile species (CCl_4 in Figs. 2, 4–7);
∞,	in the bulk of the vapor;
i,	interface;
w,	collant surface;
$'$,	designates liquid, also differentiation with respect to η;
$\bar{\ }$,	condensate.

INTRODUCTION

CONDENSATION studies in direct contact were mainly concerned with a single vapor condensing on its own coolant or with a vapor containing a noncondensable gas [1–9]. There have been, however, very few investigations [10–11] on direct contact condensation of a single vapor or mixtures on another coolant.

Unlike a miscible condensate, the phenomena occurring on the coolant surface in case of an immiscible condensate are quite complicated. In most cases they probably do not correspond to a filmwise spread of the condensate on the coolant even for the case of a single immiscible condensate.

Maa and Hickman [10], for example, condensed steam directly on a cold oil jet and were able to explain their results according to the theory of heterogeneous nucleation which assumes that the condensate nucleates in the form of tiny droplets on the coolant. More about these phenomena may be gathered from non-direct contact experiments. Sykes and Marchello [12], for example, condensed steam–toluene mixtures and others in a tube. They correlated their data by the use of a model having a continuous film of the organic liquid on the condenser surface and water drops nucleating on the top of it. The "water side" nucleation heat-transfer coefficient was found to be much lower than the one which would have been obtained had they used a two-film model with the water in laminar flow as a secondary film on the organic liquid. In other words, the effect of the thickness of the condensate is much smaller as compared to the effect of the droplets nucleation. Indeed, Bernhardt and Westwater [13] recently, using a high speed camera, observed the above behavior but found that the condensation phenomena of immiscible mixtures was even much more complicated.

In light of what has been said, the overall complicated phenomena at the vapor–liquid interface are included in the present analysis by expressing them in terms of a constant heat-transfer coefficient of the interface designated as h_i. Indeed, Tamir *et al.* [14] found that h_i is practically constant by condensing directly on water several organic vapors which are immiscible in water. In this work, the value of the interfacial resistance, namely $1/h_i$, was found appreciable and equal to the average resistance offered by the water film.

In this article we present a theoretical treatment of the direct contact condensation process of a binary vapor mixture on a coolant stream. The analysis is suitable either for immiscible or miscible condensates in the coolant. The diffusion in the vapor mixture is included in the analysis and hence a simultaneous solution of the vapor phase boundary-layer equations and that of the liquid is necessary to predict the condensation rate. On the other hand, by applying this analysis to heat-transfer measurements, it is possible to separate the total resistance, namely due to diffusion in the vapor and the phenomena occurring at the vapor–liquid interface. The latter resistance, $1/h_i$, is important because its value may shed some light on the condensation process in such systems.

MATHEMATICAL FORMULATION AND SOLUTION

In the physical model under consideration (see Fig. 1), a coolant stream at temperature T_0 is introduced into a rectangular duct or a wetted wall type condenser, with a fully developed velocity profile. A

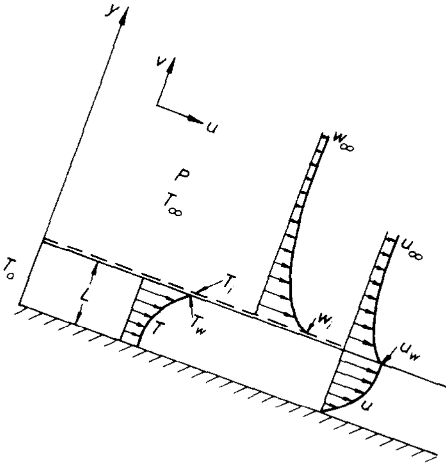

FIG. 1. Physical model and co-ordinates.

binary vapor mixture with mass fraction w_∞ of the volatile component enters at temperature $T_\infty (> T_0)$ and with a uniform velocity u_∞.

During its flow, it condenses on the laminar coolant surface. The vapors are assumed to attain the coolant surface velocity, u_w. The additional thickness due to condensate is neglected in the analysis, hence the curvature of the x-coordinate which was placed along the condensate surface is also ignored. Also owing to the small diffusivities encountered in the liquid mixture, we neglect diffusion within the liquid mixture (either in the immiscible case or when the condensate is miscible in the coolant). The condensate is assumed to be in equilibrium state at T_i with the vapor mixture in its vicinity. The vapors are assumed to behave as an ideal mixture. The energy equation in the vapor phase is discarded because the major heat in this process is transferred to the coolant as latent heat. It is also expected that due to the velocities u_w and u_∞, the buoyancy effect may be neglected and hence its term was omitted from the momentum equation.

For constant properties, the conservation equations in the vapor mixture boundary layer read

$$\frac{\partial u}{\partial x}+\frac{\partial v}{\partial y}=0 \tag{1}$$

$$u\frac{\partial u}{\partial x}+v\frac{\partial u}{\partial y}=\nu\frac{\partial^2 u}{\partial y^2} \tag{2}$$

$$u\frac{\partial w}{\partial x}+v\frac{\partial w}{\partial y}=D\frac{\partial^2 w}{\partial y^2}. \tag{3}$$

where $w = \rho_1/\rho$ corresponds to the volatile species. The energy equation in the coolant reads

$$u_w\left[1-\left(\frac{y}{L}\right)^2\right]\frac{\partial T}{\partial x}=\alpha'\frac{\partial^2 T}{\partial y^2}. \tag{4}$$

The boundary conditions are:

$$\text{at} \quad x=0: \quad T=T_0, \quad u=u_\infty, \quad w=w_\infty \tag{5}$$

$$\text{at} \quad y=\infty: \quad u=u_\infty, \quad w=w_\infty \tag{6}$$

$$\text{at} \quad y=0: \quad T=T_w, \quad u=u_w \tag{7}$$

$$\text{at} \quad y=-L: \quad \frac{\partial T}{\partial y}=0. \tag{8}$$

The matching conditions at $y = 0$ are:

$$-\rho v_i \lambda = h_i(T_i-T_w)=k'\frac{\partial T}{\partial y}. \tag{9}$$

The mass fraction of the volatile component in the condensate, $\bar{w}_i$, is the ratio between its own flux and the total condensation flux, namely,

$$\bar{w}_i=\frac{-\rho D\dfrac{\partial w}{\partial y}+\rho v_i w_i}{\rho v_i}. \tag{10}$$

The vapor–liquid equilibria relationship needed to complete the formulation may be expressed by:

$$\frac{w_i}{w_i+(1-w_i)(M_1/M_2)} = \frac{\gamma(\bar{w}_i)P^0(T_i)}{P}\times\frac{\bar{w}_i}{\bar{w}_i+(1-\bar{w}_i)(M_1/M_2)}. \tag{11}$$

The solution in the vapor phase was obtained in the coordinates (ξ, η) where

$$\xi=\frac{x\alpha'}{L^2 u_w} \qquad \eta=y\sqrt{(u_w/\nu x)} \tag{12}$$

by defining the dimensionless stream function f as

$$\psi=\sqrt{(\nu u_w x)}\,.\,f(\xi,\eta) \tag{13}$$

where ψ satisfies $u = \partial\psi/\partial y$ $v = -\partial\psi/\partial x$, equations (1) to (3) reduce to the following ordinary differential equations:

$$\tfrac{1}{2}f\frac{\partial^2 f}{\partial\eta^2}+\frac{\partial^3 f}{\partial\eta^3}=\xi\left(\frac{\partial f}{\partial\eta}\frac{\partial^2 f}{\partial\xi\partial\eta}-\frac{\partial f}{\partial\xi}\frac{\partial^2 f}{\partial\eta^2}\right) \tag{14}$$

$$\tfrac{1}{2}f\frac{\partial\phi}{\partial\eta}+Sc^{-1}\frac{\partial^2\phi}{\partial\eta^2}=\xi\left(\frac{\partial f}{\partial\eta}\frac{\partial\phi}{\partial\xi}-\frac{\partial f}{\partial\xi}\frac{\partial\phi}{\partial\eta}\right) \tag{15}$$

where

$$\phi(\xi,\eta)=w/w_\infty. \tag{16}$$

For small x, the solution in the liquid side was more conveniently obtained in the coordinates $(\xi, \tilde{\eta})$ where ξ is given by equation (12) and

$$\tilde{\eta}=\frac{y}{2L\sqrt{\xi}}. \tag{17}$$

Hence the energy equations (4) reads

$$(1-4\xi\tilde{\eta}^2)\left(\xi\frac{\partial\theta}{\partial\xi}-\frac{1}{2}\tilde{\eta}\frac{\partial\theta}{\partial\tilde{\eta}}\right)=\frac{1}{4}\frac{\partial^2\theta}{\partial\tilde{\eta}^2} \tag{18}$$

where

$$\theta(\xi,\tilde{\eta})=\frac{T-T_0}{T_\infty-T_0}. \tag{19}$$

For large values of x, (or ξ) namely when the temperature changes penetrated to the wall surface, the numerical solutions continues with equation (4) using the Crank–Nicolson procedure.

The transformed boundary conditions are:

$$\text{at} \quad \xi=0: \quad f'=\beta, \quad \phi=1, \quad \theta=0 \tag{20}$$

where

$$\beta=\frac{u_\infty}{u_w} \tag{21}$$

$$\text{at} \quad \eta=\infty: \quad f'=\beta, \quad \phi=1 \tag{22}$$

$$\text{at} \quad \eta=0: \quad f'=1, \quad f=f_i, \quad \theta=\theta_w. \tag{23}$$

Note that the differentiation is with respect to η. For small ξ we use,

$$\text{at} \quad \tilde{\eta} \to \infty: \qquad \theta = 0. \tag{24}$$

For large ξ equation (4) is solved with boundary condition (8) where a smooth merging from the $(\xi, \tilde{\eta})$ grid into the $(\xi, y/L)$ grid was performed.

The matching conditions at $\eta = 0$ are:

$$\frac{N}{2\sqrt{\xi}}\tilde{f}_i = B(\theta_i - \theta_w) = \frac{1}{2\sqrt{\xi}}\frac{\partial\theta}{\partial\tilde{\eta}} \tag{25}$$

$$\bar{w}_i = w_\infty \frac{2Sc^{-1}\dfrac{\partial f}{\partial\eta} + \tilde{f}_i\theta_i}{\tilde{f}_i} \tag{26}$$

where

$$\tilde{f}_i = f_i + 2\xi\frac{\partial f}{\partial\xi} = -2\sqrt{(\xi/K)}\,.\,V_i \tag{27}$$

$$B = \frac{h_i L}{k'} \tag{28}$$

is a dimensionless heat-transfer coefficient of the interface.

The above set of equations admits a similarity solution only for the entrance region, namely as $\xi \to 0$, and if the interfacial resistance is negligible, namely $B \to \infty$ (or $T_i = T_w$).

Under these conditions the solution yields that θ_i (or T_i) is constant and equation (18) gives for a semi-infinite body that at

$$\tilde{\eta} = 0 \quad \partial\theta/\partial\tilde{\eta} = 2\theta_i/\sqrt{\pi}.$$

Hence, from equations (25), (27)

$$\tilde{f}_i = f_i = \frac{2}{\sqrt{\pi}}\frac{\theta_i}{N} = \text{constant}. \tag{29}$$

Note that θ_i is yet unknown and is part of the solution sought. Integration of equations (14)–(16) gives:

$$f' = 1 + (\beta - 1)\frac{\displaystyle\int_0^\eta \exp\left(-0{\cdot}5\int_0^\eta f\,\mathrm{d}\eta\right)\mathrm{d}\eta}{\displaystyle\int_0^\infty \exp\left(-0{\cdot}5\int_0^\eta f\,\mathrm{d}\eta\right)\mathrm{d}\eta} \tag{30}$$

where

$$f = f_i + \int_0^\eta f'\,\mathrm{d}n. \tag{31}$$

The interfacial concentration of the volatile component, $\phi_i = w_i/w_\infty$, is

$$\phi_i = 1 + \frac{\displaystyle 0{\cdot}5\,Scf_i(\bar{w}_i/w_\infty - 1)\int_0^\infty \exp\left(-0{\cdot}5\int_0^\eta Scf\,\mathrm{d}\eta\right)\mathrm{d}\eta}{\displaystyle 0{\cdot}5\,Scf_i\int_0^\infty \exp\left(-0{\cdot}5\int_0^\eta Scf\,\mathrm{d}\eta\right)\mathrm{d}\eta - 1}. \tag{32}$$

A solution for large ξ was affected by a forward marching technique. The finite difference formulation of equations (14), (15) and (18) was obtained by a fully implicit finite difference method. If j is a node point in the η direction and the interval size is $\Delta\eta$, one obtains from (14) n algebraic equations for f, where $j = 3, \ldots, n-2$:

$$-f_{j-2} + a_j f_{j-1} + b_j f_j + c_j f_{j+1} + f_{j+2} = d_j\xi. \tag{33}$$

The a, b, c and d are obtainable in terms of known quantities of the previous step. Taking advantage of the boundary conditions yields also that

$$3f_n - 4f_{n-1} + f_{n-2} = \beta\Delta\eta \tag{34}$$

$$f_n - 2f_{n-1} + f_{n-2} = 0 \tag{35}$$

$$-3f_1 + 4f_2 - f_3 = 2\Delta\eta \tag{36}$$

$$f_1\left(-1 - 2\frac{\xi}{\Delta\xi}\right) = \tilde{f}_1 - 2\frac{\xi}{\Delta\xi}f_1^*. \tag{37}$$

$\Delta\xi$ is the interval sized in the ξ direction, where subscripts 1 and n designate values at the interface and the edge of the boundary layer, respectively. Note that $\tilde{f}_1$ is known if the interfacial conditions are known, equation (25). f_1^* designates a known value from previous step. The vapor side mass conservation equation (15) and the energy equation in the liquid (18) were also fully implicitly approximated. It yielded algebraic equations in the form suitable for the Gauss's elimination method and hence are not spelled out here. It should be noted that first derivatives in the $\eta, \tilde{\eta}$ directions were approximated from three values of adjacent node points.

The method of solution of the finite difference equations was as follows: a guess is made for θ_w, physical properties were evaluated and hence the liquid side could be solved which yielded θ_i, equation (25). This enables us to obtain $\bar{w}_i$ from the vapor liquid equilibrium relationship, equation (11). We designate this value as $\bar{w}_{i,\text{equil}}$. At this stage, physical properties for the vapor phase were calculated. It should be noted that although our analysis assumes constant properties, they were corrected at each step. As a reference temperature and concentration for properties evaluation we used 0·5 $(T_w + T_{-L})$ for the liquid, 0·5 $(T_i + T_\infty)$ and 0·5 $(w_i + w_\infty)$ for the vapor. Profiles in the vapor phase could now be calculated and hence a new value for $\bar{w}_i$ was obtained from equation (26). Defining a function $F(\theta_w) = \bar{w}_{i,\text{equil.}} - \bar{w}_i$, it was decided to stop the iteration for θ_w once $F(\theta_w)$ approached zero. It should be noted that for $B = \infty$, we used at the first step (namely, $\xi = 0$) the similarity solution given by equations (30)–(32) which were integrated numerically and solved iteratively for θ_i.

RESULTS AND DISCUSSIONS

Our solution is demonstrated for the condensation of the binary mixture CS_2–CCl_4 (carbon disulfide–carbon tetrachloride) on water at total pressure of 760 mmHg. This mixture is immiscible in water but the condensable components have a complete mutual miscibility. The physical properties of the mixtures and that of the pure components, as well as the equilibrium relationship, were evaluated by consulting references [15–18].

The results for the leading edge namely small ξ, are reported in Fig. 2. In this case the interfacial resistance was neglected, namely $B = \infty$, and hence equations (30)–(32) were applicable. $Q(B = \infty)$ is the dimensionless heat flux which is defined by the dimensionless temperature gradient, $\partial\theta/\partial\bar{\eta}$, where $Q_\infty(B = \infty)$ is the maximum heat flux evaluated when $T_i = T_\infty$. From reference [19] $Q_\infty(B = \infty) = 1/\sqrt{(\pi\xi)}$. The heat flux ratio is plotted vs the bulk temperature of the vapor mixture, starting from the boiling point of pure CS_2 up to that of CCl_4. The parameter of the curves is the maximum driving force $(T_\infty - T_0)$. The general conclusion which may be drawn from Fig. 2 is that the actual dimensionless condensation flux is lower than the maximum one. As observed also, all curves exhibit a minimum value for the heat flux ratio with a value of unity at the extreme temperatures corresponding to condensation of a pure vapor.

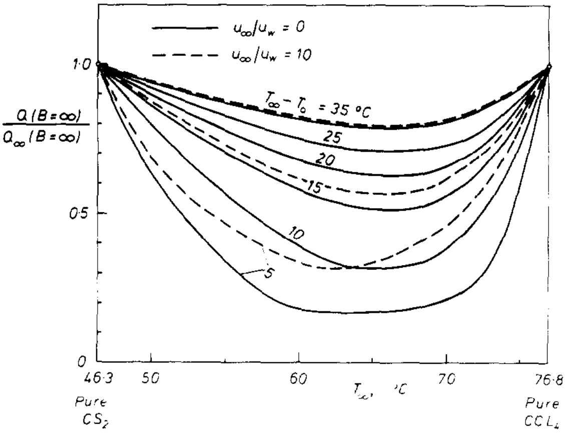

FIG. 2. Heat flux ratio for small x in condensation of CS_2–CCl_4 on H_2O ($P = 760$ mmHg).

This behavior is due to the diffusion in the vapor phase by which concentration of the more volatile component (CS_2) becomes higher at the interface as compared to its concentration in the bulk. It should be noted that this behavior is similar to condensation of a vapor in the presence of a noncondensable gas where the latter tends to accumulate at the condensing surface. The effect of the thermal driving force $(T_\infty - T_0)$ is also shown in Fig. 2 and it may be concluded that by increasing its value, the actual heat flux tends also to increase. This behavior, however, is completely opposite to the case of condensation in the presence of a noncondensable gas [20–21].

The above-mentioned trends can be explained by analyzing the following simplified model: If we assume total condensation of the vapor, mass balance yields that $\bar{w}_i = w_\infty$. By plotting this result, line AD in Fig. 3, on the equilibrium diagram T vs $\bar{w}$, w, we obtain at point B the interfacial temperature T_i. Now, we plot the T_0 line which is parallel to the T_∞ line. The heat fluxes are proportional to the temperature differences, hence $Q(B = \infty)/Q_\infty(B = \infty) = BC/AC$ explains the previous phenomena.

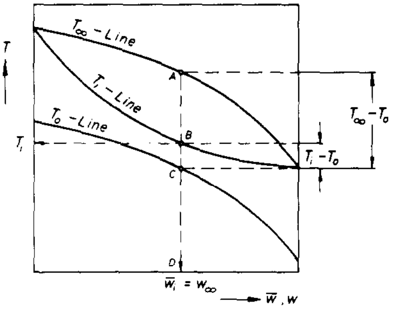

FIG. 3. Schematic equilibrium diagram.

As recalled, forced convection in the vapor phase was also included in the analysis. It is investigated only for small ξ where its influence is most pronounced. The dotted lines in Fig. 2 demonstrate this effect, where u_∞ was chosen ten times higher than the liquid surface velocity u_w. Since $Q_\infty(B = \infty)$ is unaffected by forced convection, we may observe that forced convection is appreciable only for relatively small values of $(T_\infty - T_0)$ where for large differences, for example 35 degC, it is negligible.

The effect of the surface resistance (inversely proportional to B) on the condensation heat transfer is illustrated in Figs. 4 and 5. Figure 4 corresponds to bulk conditions at saturation temperature of 65°C, whereas for Fig. 5 the saturation bulk temperature is 76°C which corresponds to very low concentration of the more volatile component (CS_2 with $w_\infty = 0{\cdot}0121$). Note that Q corresponds to the actual local flux in the presence of surface resistance where $Q(B = \infty)$ is the local heat flux when the interfacial resistance is negligible. As expected, the effect of the surface resistance is appreciable at the entrance region where the heat flux ratio is lower than unity. Note that at $\xi = 0$,

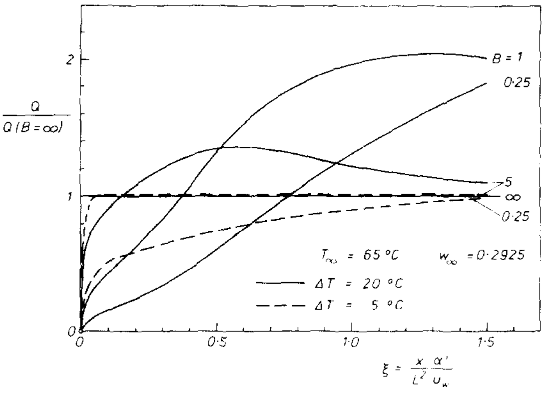

FIG. 4. Effect of surface resistance $(1/B)$ on heat flux ratio in condensation of CS_2–CCl_4 on H_2O at 65°C.

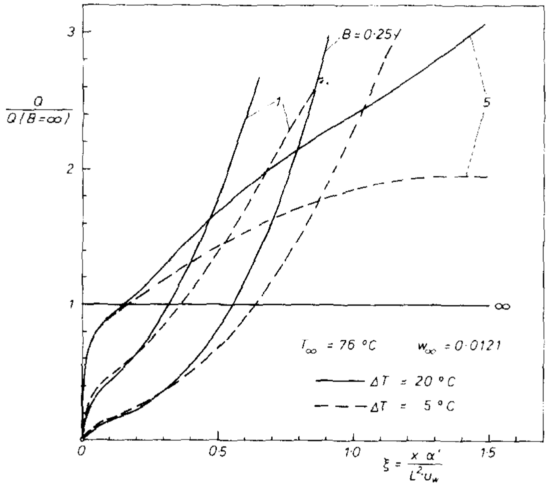

FIG. 5. Effect of surface resistance $(1/B)$ on heat flux ratio in condensation of CS_2–CCl_4 at 76°C.

$Q = B$ while $Q(B = \infty) = \infty$; hence the heat flux ratio must be zero at $\xi = 0$ for all finite values of B. In general it is also observed that as ξ increases, the local heat-transfer ratio also increases and might reach values much higher than unity, but as $\xi \to \infty$ it must approach unity. This phenomenon is also accentuated in condensation of almost a pure vapor, as CCl_4 in Fig. 4 with bulk contraction of 0·9879. This behavior is explained as follows: *if the condensation unit is long enough, the coolant must eventually reach the saturation temperature of the condensing vapor and the total amount of heat delivered to the coolant is proportional to* $\int_0^\infty Q\,d\xi$. However, at the leading edge $Q \approx B$ and is lower than $Q_\infty(B = \infty)$ which means it must be higher for higher values of ξ. This explains also the maximum in the heat flux ratio versus ξ which is clearly observed in Fig. 4 for $B = 5$. A practical conclusion which may be drawn from this discussion is that the effect of the high surface resistance is indeed appreciable on short ducts rather than on long ones. For long ducts, of course, the integrated condensation rate must be independent of the value of the interfacial resistance.

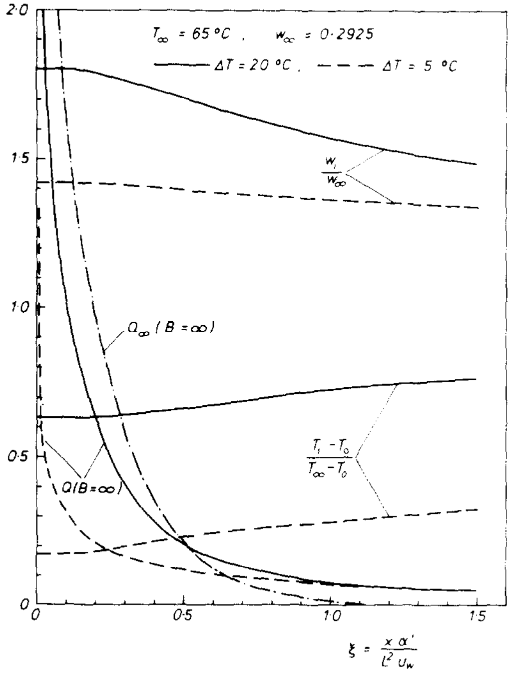

FIG. 6. Variation along ξ of the interfacial concentration, temperature and heat flux for $B = \infty$ and $T_\infty = 65$°C.

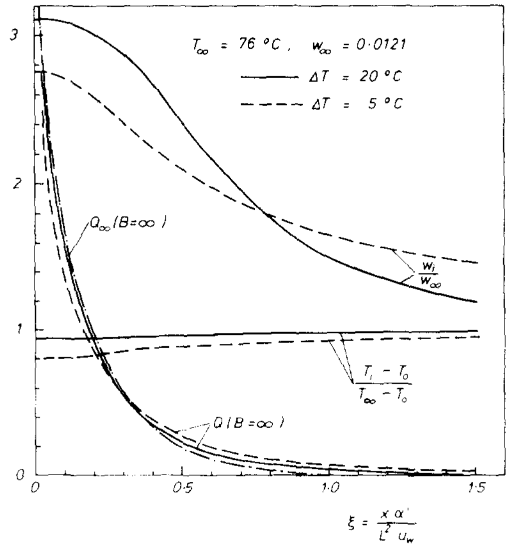

FIG. 7. Variation along ξ of the interfacial concentration, temperature and heat flux for $B = \infty$ and $T_\infty = 76$°C.

Figures 6 and 7, corresponding to $B = \infty$, provide typical variations of the interfacial temperature and concentration as well as $Q(B = \infty)$ with ξ. The latter makes it possible to calculate the actual condensation flux Q with the aid of Figs. 4 and 5 once the value of B is known or vice versa. An important conclusion with regard to the range of validity of the similarity solution ($B = \infty$) may be drawn from the temperature profiles. As recalled, the similarity solution yields θ_i = constant (equation 29) for the entrance region. The curves show that this result may practically be applicable up to $\xi = 0{\cdot}1$. Note in Fig. 7 that all Q's are quite identical for small ξ as compared to Fig. 6. This is because the bulk concentration of the volatile material is low and corresponds to almost condensation of a pure component, namely CCl_4 with boiling point of 76·8°C.

Theoretical results for condensation of binary mixtures were also reported by Sparrow [22], Denny [23] and Marschall [24]. They considered the case of film condensation on a cooled wall rather than direct contact. However, the general trends which were observed are similar.

Acknowledgements—This work was performed while the first two authors stayed at the University of Karlsruhe, Lehrstuhl und Institut fur Thermische Verfahrenstechnik Prof. Dr.-Ing. E. U. Schlunder. The sponsorship of the DAAD is greatly acknowledged.

REFERENCES

1. D. Hasson, D. Luss and R. Peck, Theoretical analyses of vapour condensation on laminar liquid jets, *Int. J. Heat Mass Transfer* 7, 969 (1964).
2. D. Hasson, D. Luss and U. Navon, An experimental study of steam condensation on a laminar water sheet, *Int. J. Heat Mass Transfer* 7, 983 (1964).
3. J. R. Maa, Condensation studies with the jet stream tensimeter, *I/EC Fundamentals* **8**, 564 (1969).
4. J. R. Maa, Rates of evaporation and condensation between pure liquids and their own vapor, *I/EC Fundamentals* 9, 283 (1970).
5. D. T. Jamieson, The condensation coefficient of water, NEL Report No. 168, East Kilbride, Glasgow (May 1965).
6. A. Tamir and D. Hasson, Evaporation and condensation coefficient of water, *Chem. Engng Jl* **2**, 200 (1971).
7. A. Kogan and M. Victor, Some aspects of flash distillation without metallic surfaces, *Desalination* **4**, 80 (1968).
8. S. E. Sadek, Condensation of steam in the presence of air. Experimental mass transfer coefficient in a direct-contact, *I/EC Fundamentals* 7, 321–324 (1968).
9. A. Tamir and Y. Taitel, Improving condensation rate by interfacial suction and forced convection in the presence of noncondensable gases, *Israel J. Technol.* **9**, 69 (1971).
10. J. R. Maa and K. Hickman, Direct condensation of steam on a modified oil coolant, *Desalination* **10**, 95 (1972).
11. S. L. Goren and G. R. Wilke, Sea water conversion laboratory report No. 67–1, Water resources center, Desalination report No. 14, 31 (1967).
12. J. A. Sykes and J. M. Marchello, Condensation of immiscible liquids on horizontal tube, *I/EC Process. Des. Dev.* **9**, 63 (1970).
13. S. H. Bernhardt, J. J. Sheridan and J. W. Westwater, Condensation of immiscible mixtures, *A.I.Ch.E. Symp. Ser.* **68**, 21 (1972).
14. A. Tamir and Y. Rachmilev, Direct contact condensation of an immiscible vapor on a thin film of water, *Int. J. Heat Mass Transfer* **17**(10), 1241–1251 (1974).
15. *VDI-Wärmeatlas*, Deutscher Ingenieur, Dusseldorf (1953).
16. J. H. Perry, *Chemical Engineering Handbook*, 4th Edn. McGraw-Hill, New York (1963).
17. R. C. Reid and T. K. Sherwood, *The Properties of Gases and Liquids*. McGraw-Hill, New York (1966).
18. E. Hala *et al.*, *Vapor–Liquid Equilibrium Data at Normal Pressures*, 1st Edn. Pergamon Press, Oxford (1968).
19. H. S. Carslaw and J. C. Jaeger, *Conduction of Heat in Solids*. Oxford University Press, London (1959).
20. E. M. Sparrow and S. H. Lin, Condensation heat transfer in the presence of a noncondensable gas, *J. Heat Transfer* **86C**, 430–436 (1964).
21. W. J. Mincowycz and E. M. Sparrow, Condensation heat transfer in the presence of a noncondensable, interfacial resistance, superheating, variable properties, and diffusion, *Int. J. Heat Mass Transfer* **9**, 1125–1144 (1966).
22. E. M. Sparrow and E. Marschall, Binary gravity-flow film condensation, *J. Heat Transfer* **91C**, 205 (1969).
23. V. E. Denny and V. J. Jusionis, Effects of forced flow and variable properties on binary film condensation, *Int. J. Heat Mass Transfer* **15**, 2143 (1972).
24. E. Marshall and R. S. Hickman, Laminar gravity-flow film condensation of binary vapor mixtures of immiscible liquids, an ASME publication, paper No. 72-WA/HT-8 (1972).

CONDENSATION DES MELANGES BINAIRES PAR CONTACT DIRECT

Résumé—On présente une analyse, de type couche limite, de la condensation des mélanges binaires de vapeur par contact direct avec un réfrigérant en écoulement laminaire dans une conduite. Le condensat du mélange binaire peut être miscible ou non avec le réfrigérant. Néanmoins les deux composants condensables sont supposés complètement miscibles. L'analyse inclut aussi les effets de la convection de la vapeur et de la résistance à l'interface vapeur–liquide. L'analyse suppose des propriétés constantes qui sont évaluées à un état de référence approprié.

L'équation de couche limite est résolue numériquement dans un système transformé de coordonnées qui admet une solution affine pour les conduites courtes quand la résistance est négligeable ($B = \infty$).

La solution est obtenue pour la condensation du mélange CS_2–CCl_4, non miscible dans l'eau.

Dans le cas où B est infini au bord d'attaque, l'analyse prévoit une réduction appréciable des flux de condensation comparés aux valeurs maximales obtenues quand la température moyenne de la vapeur existe à l'interface. Cette réduction dépend de la composition du mélange et de $(T_\infty - T_0)$. L'effet de la convection forcée est trouvé sensible seulement pour des valeurs relativement faible de $(T_\infty - T_0)$. L'effet de la résistance de surface est appréciable près du bord d'attaque. Les résultats indiquement aussi que la solution affine peut être étendue jusqu'à $\xi = 0, 1$.

KONDENSATION VON BINÄREN GEMISCHEN DURCH DIREKTEN KONTAKT

Zusammenfassung—Die vorliegende Arbeit stellt eine Grenzschichtbetrachtung bei der Kondensation von binären Gemischen durch direkten Kontakt mit laminar fließender Kühlflüssigkeit im Rohr dar. Das Kondensat des binären Gemischs kann mit der Kühlflüssigkeit mischbar sein oder nicht. Es wird aber angenommen, daß beide Komponenten des Kondensats miteinander vollkommen mischbar sind. Die Betrachtung schließt ebenso die Wirkung der erzwungenen Konvektion des Dampfes ein wie auch den Widerstand an der Grenzschicht zwischen Dampf und Flüssigkeit. Es werden konstante Eigenschaften angenommen, die auf einen entsprechenden Zustand bezogen werden. Die Gleichungen für die Grenzschicht wurden in einem transformierten Koordinatensystem numerisch gelöst, welches eine Lösung durch Ähnlichkeitsbetrachtungen für kurze Rohre und einen vernachlässigbaren Oberflächenwiderstand gestattet ($B = \infty$). Die Lösung wird für die Kondensation des unlöslichen Gemisches CS_2–CCL_4 auf Wasser unter atmosphärischem Druck vorgeführt.

Für den Fall $B = \infty$ und an der Anlaufseite wird eine merkliche Erniedrigung des Kondensatanfalls vorausgesagt, verglichen mit den maximalen Werten, die gewonnen werden, wenn die Temperaturen im Dampfkern und an der Grenzschicht gleich sind. Diese Erniedrigung hängt von der Zusammensetzung des Gemischs und vom Maximum des thermischen Potentials $(T_\infty - T_0)$ ab. Die Wirkung der erzwungenen Konvektion ist nur für verhältnismäßig kleine Werte von $(T_\infty - T_0)$ erheblich. Die Wirkung des Oberflächenwiderstandes ist in der Nähe der Anlaufseite beachtlich. Die Ergebnisse zeigen ebenfalls, daß die Ähnlichkeitslösung bis zu $\xi = 0{,}1$ ausgedehnt werden kann.

НЕПОСРЕДСТВЕННАЯ КОНТАКТНАЯ КОНДЕНСАЦИЯ БИНАРНЫХ СМЕСЕЙ

Аннотация — Анализируется пограничный слой при непосредственной контактной конденсации бинарных смесей пара на поверхности теплоносителя при его ламинарном течении в трубе. Конденсат бинарной смеси может не смешиваться или смешиваться с теплоносителем. Однако, предполагается, что оба конденсируемых компонента полностью смешиваются. При анализе учитывается влияние вынужденной конвекции и сопротивления на поверхности раздела: пар-жидкость. Предполагается, что оцениваемые в соответствующем начальном состоянии свойства постоянны.

Уравнение пограничного слоя решено численно в преобразованной системе координат, где для коротких труб взято решение подобия и принято, что поверхностное сопротивление пренебрежимо мало ($B = \infty$).

Применение решения показано на примере конденсации несмешивающейся смеси CS_2—CCl_4 на поверхности воды при атмосферном давлении.

При $B = \infty$ аналитический расчет для передней кромки дает значительное уменьшение потока конденсата по сравнению с максимальными значениями, полученными в случае наличия на поверхности раздела среднемассовой температуры пара.

Эко уменьшение зависит от состава смеси и максимальной тепловой движущейся силы $(T_\infty - T_0)$. Влияние вынужденной конвекции является существенным только в случае относительно малых значений $(T_\infty - T_0)$. Поверхностное сопротивление оказывает значительное влияние вблизи передней кромки. Полученные результаты также показывают, что решение подобия может быть применено к случаю $\xi = 0{,}1$.